

# Analyses of Type Ia Supernova Data in Cosmological Models with a Local Void

K. Tomita

*Yukawa Institute for Theoretical Physics, Kyoto University, Kyoto, 606-8502, Japan*

2 December 2024

## ABSTRACT

The data of type Ia supernovae observed by the High- $z$  SN Search Team and Supernova Cosmology Project are analyzed in inhomogeneous cosmological models with a local void on scales of about 200 Mpc, to derive the best-fit values of model parameters and the confidence contours. The  $\chi^2$  fitting is found to be slightly better than that in homogeneous models. It is shown that (1) the best-fit values are most sensitive to the ratio  $R$  of the outer Hubble constant ( $H_0^{\text{II}}$ ) to the inner Hubble constant ( $H_0^{\text{I}}$ ), (2) the best-fit outer density parameter ( $\Omega_0^{\text{II}}$ ) (and cosmological constant parameter ( $\lambda_0^{\text{II}}$ )) increases (and decreases) with the increase of  $R$ , respectively, and (3) ( $\Omega_0^{\text{II}}, \lambda_0^{\text{II}}$ ) can be (1, 0) for  $R \approx 0.8$ .

**Key words:** cosmology: observations – large-scale structure of Universe

## 1 INTRODUCTION

Nowadays the most important cosmological observations are the [magnitude  $m$  - redshift  $z$ ] relation of type Ia supernovae (SNIa) and the CMB anisotropy. In the former observations, SNIa play a role of best standard candles and two groups, the High- $z$  SN Search Team (Schmidt et al. 1998; Riess et al. 1998) and the Supernova Cosmology Project (Perlmutter et al. 1999) have so far observed 50 and 60 SNIa, respectively. From their results it was suggested that a significant dark energy content fills our universe under the assumption of its homogeneity and isotropy.

On the other hand, inhomogeneous models with a local void on scales of about 200 Mpc were studied by the present author (Tomita 2000a) in connection with the puzzling behavior of cosmic bulk flows (Hudson et al. (1999) and Willick (1999)), and the possibility that the accelerating behavior of high- $z$  SNIa in  $[m, z]$  relation may be explained without cosmological constant was shown subsequently (Tomita 2000b). A historical survey of works concerned with local voids can be seen in one of previous papers (Tomita 2001a). Since these inhomogeneous models include many parameters (such as the inner and outer values of the Hubble constant and density parameter, cosmological constant and the boundary radius), we have recently examined the dependence of the above relation on these parameters, in comparison with the relations in homogeneous models with  $(\Omega_0, \lambda_0) = (0.3, 0.7)$  and  $(0.3, 0.0)$  (Tomita 2001b).

From the observational viewpoint, recent galactic redshift surveys (Marinoni et al. 1999, Marzke et al. 1998, Folkes et al. 1999, Zucca et al. 1997) show that in the region around  $200 - 300h^{-1}$  Mpc from us the distribution of galaxies may

be inhomogeneous. Moreover, a large-scale inhomogeneity suggesting a wall around the void on scales of  $\sim 250h^{-1}$  Mpc has recently been found by Blanton et al. (2000) in the SDSS commissioning data. Similar walls on scales of  $\sim 250h^{-1}$  Mpc have already been found in the Las Campanas and 2dF redshift surveys near the Northern and Southern Galactic Caps (Shectman et al. 1996, Folkes et al. 1999, Cole et al. 2000). These results may mean that there is a local void with the radius of  $200 - 300h^{-1}$  Mpc and we live in it.

In this paper we analyze directly the SNIa data of the above two groups in our inhomogeneous models with a local void on scales of about 200 Mpc, and show the confidence contours as well as the best-fit values of the model parameters. In §2 we give the basic formulation of distance modulus and the  $\chi^2$  square for statistical fitting, and in §3 show the best-fit values of model parameters and confidence contours. In §4 discussions and concluding remarks are described.

## 2 DISTANCE MODULUS AND THE $\chi^2$ SQUARE

The theoretical distance modulus is defined by

$$\mu_0^p = 5 \log \left( d_L / \text{Mpc} \right) + 25, \quad (1)$$

where  $d_L$  is the luminosity distance related to the angular-diameter distance  $d_A$  by

$$d_L = (1 + z)^2 d_A \quad (2)$$

along the light ray to a source S with the redshift  $z$ . This distance modulus is compared with the observed one given by

$$\mu_0 = m_B - M_B, \quad (3)$$

where  $M_B$  and  $m_B$  are the peak absolute magnitude and the corresponding apparent magnitude of a standard SNIa in the B band, respectively.

In this paper we consider spherical inhomogeneous cosmological models which consist of the inner homogeneous region ( $V^I$ ) and the outer homogeneous region ( $V^{II}$ ) with the boundary of radius  $\sim 200$  Mpc. The observer's position O deviates generally from the center C, but is assumed to be comparatively close to C. For the off-center observer, the angular-diameter distance  $d_A$  depends not only on  $z$ , but also the angle between the vectors  $\overline{CO}$  and  $\overline{CS}$ , where S is the source. In our previous papers (Tomita 2000a, b) the behavior of distances for off-center observers was studied. Since the angular dependence is small for remote sources, however, we can neglect it for simplicity, assuming that we are approximately at the center. Then  $d_A$  depends on the source redshift  $z$ , the inner and outer Hubble constants  $H_0^I$  and  $H_0^{II}$ , the inner and outer density parameters  $\Omega_0^I$  and  $\Omega_0^{II}$ , the outer  $\Lambda$  parameter  $\lambda_0^{II}$ , and the boundary redshift  $z_1$ . The inner  $\Lambda$  parameter  $\lambda_0^I$  is related to  $\lambda_0^{II}$  by  $\lambda_0^I = \lambda_0^{II} (H_0^{II}/H_0^I)^2$ . The equation to be solved for deriving  $d_A$  and the junction conditions were shown in Eqs. (5) - (11) in a previous paper (Tomita 2001b).

The best-fit values of the cosmological parameters are determined using the  $\chi$  square :

$$\chi^2 = \sum_i \left[ \mu_{0,i}^p(z_i | H_0^I, H_0^{II}, \Omega_0^I, \Omega_0^{II}, \lambda_0^{II}, z_1) - \mu_{0,i} \right]^2 / (\sigma_{\mu_{0,i}}^2 + \sigma_{mz,i}^2), \quad (4)$$

where  $\sigma_{\mu_0}$  is the measurement error of the distance modulus and  $\sigma_{mz}$  is the dispersion in the distance modulus corresponding to the dispersion of galaxy redshift  $\sigma_z$  (coming from peculiar velocity and uncertainty).  $\sigma_{mz}$  is related to  $\sigma_z$  as

$$\sigma_{mz} = \frac{5}{\ln 10} \left( \frac{1}{d_L} \frac{\partial d_L}{\partial z} \right). \quad (5)$$

Next the probability distribution function (PDF) is necessary to derive the confidential contours as well as the most likely values of model parameters. It is expressed as

$$p(H_0^I, H_0^{II}, \Omega_0^I, \Omega_0^{II}, \lambda_0^{II}, z_1 | \mu_0) \propto \exp(-\frac{1}{2} \chi^2), \quad (6)$$

which is consistent with Eq.(9) in Riess et al. (1998).

In the present inhomogeneous models there are six parameters and it is too complicated to consider all of them at the same time. So we treat here several cases with specific values of  $z_1, H_0^{II}/H_0^I$ , and  $\Omega_0^I$ . Then the corresponding normalized PDF is expressed as

$$p(H_0^I, \Omega_0^{II}, \lambda_0^{II} | \mu_0) = \frac{\exp(-\frac{1}{2} \chi^2)}{\int_{-\infty}^{\infty} dH_0^I \int_{-\infty}^{\infty} d\lambda_0^{II} \int_{\Omega_{0l}}^{\infty} \exp(-\frac{1}{2} \chi^2) d\Omega_0^{II}} \quad (7)$$

for given  $z_1, H_0^{II}/H_0^I$ , and  $\Omega_0^I$ , where  $\mu_0$  is the used set of distance moduli and  $\Omega_{0l}$  is the assumed lower limit of  $\Omega_0^{II}$ , being 0 or  $-\infty$ . Physically the region of  $\Omega_0^{II} < 0$  is meaningless, while it is significant statistically. To see the probability distribution independent of  $H_0^I$ , we can consider the following quantity:

$$p(\Omega_0^{II}, \lambda_0^{II} | \mu_0) = \int_{-\infty}^{\infty} p(H_0^I, \Omega_0^{II}, \lambda_0^{II} | \mu_0) dH_0^I. \quad (8)$$

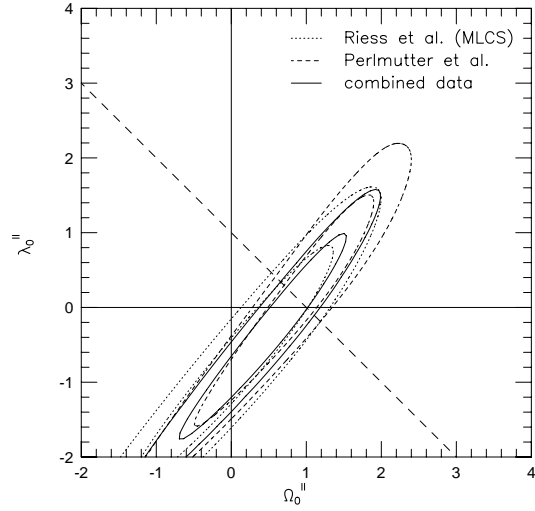


**Figure 1.** 68.3 % and 95.4 % confidence contours in the  $\Omega_0^{II} - \lambda_0^{II}$  plane in the case of  $(z_1, H_0^{II}/H_0^I, \Omega_0^I) = (0.080, 0.82, A)$ . The dotted lines represent the Riess et al. (1998) data, the dashed lines represent the Perlmutter et al (1999) data, and the solid lines represent the combined data.

The contours are drawn due to  $p(\Omega_0^{II}, \lambda_0^{II} | \mu_0)$ .

### 3 SUPERNOVA DATA AND THE FITTING

At present we have two SNIa data to be used for determining cosmological parameters: data of HSST (Schmidt et al. 1998; Riess et al. 1998) with 50 SNIa, and the data of SCP (Perlmutter et al. 1999) with 60 SNIa. 18 SNIa are common to both data.

In the former, there are two types of  $\mu_0$  data : data due to the Multicolor Light Curve Shape method (MLCS) and the template-fitting method. In each method we can use the data of  $z_i, \mu_{0,i}$  and  $\sigma_{\mu_{0,i}}$  (for  $i = 1 - 50$ ) given in their Tables. Following Riess et al. (1998) for  $\sigma_z$ , we adopt  $\sigma_z = 200 \text{ km s}^{-1}$  and add  $2500 \text{ km s}^{-1}$  in quadrature to  $\sigma_z$  for SNIa whose redshifts were determined from broad features in the SN spectrum.

In Perlmutter et al.'s paper, the data of  $m_{B,i}^{\text{eff}}, z_i, \sigma_{mz,i}$  and  $\sigma_{z,i}$  ( $i = 1 - 60$ ) were shown, but the direct values of  $\mu_{0,i}$  were not published and cannot be used. As was shown by Wang (2000), however, we have for 18 SNIa common to two teams

$$M_B^{\text{MLCS}} \equiv m_B^{\text{eff}} - \mu_0^{\text{MLCS}} = -19.33 \pm 0.25, \quad (9)$$

where  $m_B^{\text{eff}}$  is the effective B-band magnitude of SNIa given

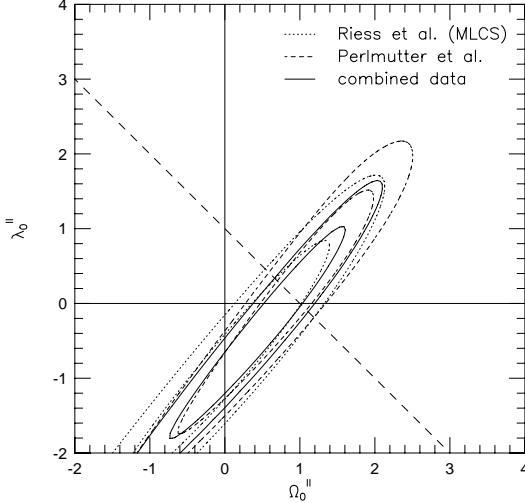


**Figure 2.** 68.3 % and 95.4 % confidence contours in the  $\Omega_0^{\text{II}} - \lambda_0^{\text{II}}$  plane in the case of  $(z_1, H_0^{\text{II}}/H_0^{\text{I}}, \Omega_0^{\text{I}}) = (0.080, 0.82, \text{B})$ .

by Perlmutter et al., and  $\mu_0^{\text{MLCS}}$  is the corresponding data of  $\mu_0$  due to MLCS method in Riess et al. (1998).

For the corrected B-band peak absolute magnitude given by Hammuy et al. (1996), on the other hand, we have

$$M_B^{\text{MLCS}} - M_B^{\text{H96}} = -0.047 \pm 0.270 \quad (10)$$

which is small enough, compared with the counterpart due to the template-fitting method. Accordingly we adopt the MLCS data among Riess et al. two data, and derive the values of  $\mu_0$  in Perlmutter et al.'s data using the relation

$$\mu_0 = m_B^{\text{eff}} - \bar{M}_B \text{ with } \bar{M}_B = -19.33 \quad (11)$$

following Wang (2000).

From the two data sets we can make a combined data consisting of 50 SNIa (from Riess et al.) and 42 SNIa (from Perlmutter et al.), where Riess et al. data are used for 18 common data (due to Wang (2000)'s procedure).

The above three kinds of data are compared with the theoretical models with the following conditions about  $z_1, H_0^{\text{II}}/H_0^{\text{I}}$ , and  $\Omega_0^{\text{I}}$ . For  $z_1$ , we adopt mainly  $z_1 = 0.080$  corresponding to the radius  $240/h^{\text{I}}$  Mpc, where  $H_0^{\text{I}} = 100h^{\text{I}}$   $\text{km s}^{-1}$   $\text{Mpc}^{-1}$ , and compare PDF in this case later with PDF in cases with  $z_1 = 0.067$  ( $cz_1/H_0^{\text{I}} = 200/h^{\text{I}}$  Mpc) and  $0.100$  ( $300/h^{\text{I}}$  Mpc). For  $H_0^{\text{II}}/H_0^{\text{I}}$ , we consider three cases with  $H_0^{\text{II}}/H_0^{\text{I}} = 0.80, 0.82$  and  $0.87$  or  $H_0^{\text{I}}/H_0^{\text{II}} = 0.25, 1.20$  and  $1.15$ , respectively.

For  $\Omega_0^{\text{I}}$ , we adopt firstly the inner low-density case (A) in which

$$\Omega_0^{\text{I}} = 0.3 \text{ for } \Omega_0^{\text{II}} > 0.6 \quad (12)$$

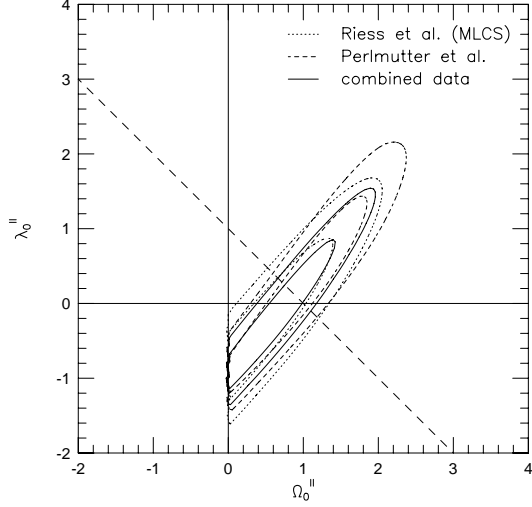


**Figure 3.** 68.3 % and 95.4 % confidence contours in the  $\Omega_0^{\text{II}} - \lambda_0^{\text{II}}$  plane in the case of  $(z_1, H_0^{\text{II}}/H_0^{\text{I}}, \Omega_0^{\text{I}}) = (0.080, 0.82, \text{A})$  with  $\Omega_{0l} = 0$ .

and

$$\Omega_0^{\text{I}} = \Omega_0^{\text{II}}/2 \text{ for } \Omega_0^{\text{II}} < 0.6. \quad (13)$$

For a comparison we consider the equi-density case (B) with

$$\Omega_0^{\text{I}} = \Omega_0^{\text{II}}/2 \left( H_0^{\text{II}}/H_0^{\text{I}} \right)^2. \quad (14)$$

Since  $\rho_0^j \propto (H_0^j)^2 \Omega_0^j$  ( $j = \text{I}, \text{II}$ ), we have  $\rho_0^{\text{I}} = \rho_0^{\text{II}}$  in this case.

In Figures 1, 2, 3, 4 and 5, we show the 68.3 % and 95.4 % confidence contours in the  $\Omega_0^{\text{II}} - \lambda_0^{\text{II}}$  plane. In Figures 1, 2 and 3, we use three kinds of data and treat the three cases in which  $(z_1, H_0^{\text{II}}/H_0^{\text{I}}, \Omega_0^{\text{I}}) = (0.080, 0.82, \text{A}), (0.080, 0.82, \text{B}),$  and  $(0.080, 0.82, \text{A})$  with  $\Omega_{0l} = 0$ , respectively. Only in the case with  $\Omega_{0l} = 0$ , the region of  $\Omega_0^{\text{II}} < 0$  is excluded. It is found comparing these figures that the difference between two cases A and B is small, and similarly the difference between two cases with  $\Omega_{0l} = -\infty$  and 0 is also small.

In Figs. 4 and 5, we show the difference in the contours in the cases with  $R \equiv H_0^{\text{II}}/H_0^{\text{I}} = 0.80, 0.82$  and  $0.87$  and  $z_1 = 0.067, 0.080$  and  $0.100$ , respectively, using the combined data. It is interesting that, as  $R$  decreases, the contours move to the direction of larger  $\Omega_0^{\text{II}}$  and smaller  $\lambda_0^{\text{II}}$ , and for  $R = 0.80$  the flat case with vanishing cosmological constant (the Einstein-de Sitter model) can be at the center of the contours.

In Table 1 the best-fit values of cosmological parameters in homogeneous models are listed for a later comparison. In Table 2, 3 and 4, we show the best-fit values of  $h^{\text{I}}, \Omega_0^{\text{II}}$  and

**Table 1.** Determined model parameters in homogeneous models.  $\chi^2_\nu$  is  $\chi^2$  per degree of freedom.  $H_0 = 100h \text{ km s}^{-1} \text{ Mpc}^{-1}$ . The errors of  $h$  represent only statistical ones.

data	Riess et al.	Perlmutter et al.	combined
$h$	$0.65 \pm 0.01$	$0.666 \pm 0.02$	$0.65 \pm 0.01$
$\Omega_0$	$0.2 \pm 0.6$	$1.0 \pm 0.4$	$0.7 \pm 0.4$
$\lambda_0$	$0.7 \pm 0.8$	$1.7 \pm 0.6$	$1.2 \pm 0.5$
$\chi^2_\nu$	1.11	1.57	1.45

**Table 2.** Determined model parameters in the case of  $(z_1, H_0^{\text{II}}/H_0^{\text{I}}, \Omega_0^{\text{I}}) = (0.080, 0.80, \text{A})$ .  $\chi^2_\nu$  is  $\chi^2$  per degree of freedom.  $H_0^{\text{I}} = 100h^{\text{I}} \text{ km s}^{-1} \text{ Mpc}^{-1}$ . The errors of  $h^{\text{I}}$  represent only statistical ones.

data	Riess et al.	Perlmutter et al.	combined
$h^{\text{I}}$	$0.64 \pm 0.01$	$0.64 \pm 0.02$	$0.64 \pm 0.01$
$\Omega_0^{\text{II}}$	$0.1 \pm 0.7$	$0.9 \pm 0.6$	$0.5 \pm 0.5$
$\lambda_0^{\text{II}}$	$-0.9 \pm 1.0$	$-0.1 \pm 0.8$	$-0.5 \pm 0.7$
$\chi^2_\nu$	1.05	1.62	1.42
$(\Omega_0^{\text{II}})_{\text{flat}}$	$1.0 \pm 0.2$	$1.0 \pm 0.2$	$1.0 \pm 0.1$

**Table 3.** Determined model parameters in the case of  $(z_1, H_0^{\text{II}}/H_0^{\text{I}}, \Omega_0^{\text{I}}) = (0.080, 0.82, \text{A})$ .  $\chi^2_\nu$  is  $\chi^2$  per degree of freedom.  $H_0^{\text{I}} = 100h^{\text{I}} \text{ km s}^{-1} \text{ Mpc}^{-1}$ . The errors of  $h^{\text{I}}$  represent only statistical ones.

data	Riess et al.	Perlmutter et al.	combined
$h^{\text{I}}$	$0.64 \pm 0.01$	$0.64 \pm 0.02$	$0.64 \pm 0.01$
$\Omega_0^{\text{II}}$	$0.1 \pm 0.7$	$0.9 \pm 0.7$	$0.6 \pm 0.5$
$\lambda_0^{\text{II}}$	$-0.7 \pm 1.1$	$0.1 \pm 1.0$	$-0.2 \pm 0.7$
$\chi^2_\nu$	1.05	1.61	1.42
$(\Omega_0^{\text{II}})_{\text{flat}}$	$0.9 \pm 0.2$	$0.9 \pm 0.2$	$0.9 \pm 0.1$

**Table 4.** Determined model parameters in the case of  $(z_1, H_0^{\text{II}}/H_0^{\text{I}}, \Omega_0^{\text{I}}) = (0.080, 0.87, \text{A})$ .  $\chi^2_\nu$  is  $\chi^2$  per degree of freedom.  $H_0^{\text{I}} = 100h^{\text{I}} \text{ km s}^{-1} \text{ Mpc}^{-1}$ . The errors of  $h^{\text{I}}$  represent only statistical ones.

data	Riess et al.	Perlmutter et al.	combined
$h^{\text{I}}$	$0.64 \pm 0.01$	$0.65 \pm 0.02$	$0.64 \pm 0.01$
$\Omega_0^{\text{II}}$	$0.2 \pm 1.0$	$0.7 \pm 0.7$	$0.6 \pm 0.6$
$\lambda_0^{\text{II}}$	$-0.2 \pm 1.1$	$0.7 \pm 1.1$	$0.3 \pm 0.8$
$\chi^2_\nu$	1.05	1.61	1.42
$(\Omega_0^{\text{II}})_{\text{flat}}$	$0.7 \pm 0.2$	$0.7 \pm 0.2$	$0.7 \pm 0.1$

**Table 5.** Determined model parameters in the case of  $(z_1, H_0^{\text{II}}/H_0^{\text{I}}, \Omega_0^{\text{I}}) = (0.080, 0.82, \text{B})$ .  $\chi^2_\nu$  is  $\chi^2$  per degree of freedom.  $H_0^{\text{I}} = 100h^{\text{I}} \text{ km s}^{-1} \text{ Mpc}^{-1}$ . The errors of  $h^{\text{I}}$  represent only statistical ones.

data	Riess et al.	Perlmutter et al.	combined
$h^{\text{I}}$	$0.64 \pm 0.01$	$0.64 \pm 0.02$	$0.64 \pm 0.01$
$\Omega_0^{\text{II}}$	$0.0 \pm 0.7$	$0.8 \pm 0.7$	$0.5 \pm 0.5$
$\lambda_0^{\text{II}}$	$-0.8 \pm 1.1$	$0.0 \pm 1.0$	$-0.3 \pm 0.8$
$\chi^2_\nu$	1.05	1.62	1.42
$(\Omega_0^{\text{II}})_{\text{flat}}$	$0.9 \pm 0.2$	$0.9 \pm 0.2$	$0.9 \pm 0.1$

**Table 6.** Determined model parameters in the case of  $(z_1, H_0^{\text{II}}/H_0^{\text{I}}, \Omega_0^{\text{I}}) = (0.080, 0.82, \text{A})$ .  $\chi_{\nu}^2$  is  $\chi^2$  per degree of freedom.  $H_0^{\text{I}} = 100h^{\text{I}}$  km s $^{-1}$  Mpc $^{-1}$ . The errors of  $h^{\text{I}}$  represent only statistical ones.

data	Riess et al.	Riess et al.	combined	combined
$z_1$	0.067	0.100	0.067	0.100
$h^{\text{I}}$	$0.64 \pm 0.01$	$0.64 \pm 0.01$	$0.64 \pm 0.01$	$0.64 \pm 0.01$
$\Omega_0^{\text{II}}$	$-0.3 \pm 0.7$	$0.4 \pm 0.7$	$0.2 \pm 0.5$	$0.9 \pm 0.5$
$\lambda_0^{\text{II}}$	$-1.3 \pm 1.1$	$-0.3 \pm 1.1$	$-0.7 \pm 0.8$	$0.2 \pm 0.8$
$\chi_{\nu}^2$	1.10	1.13	1.45	1.46

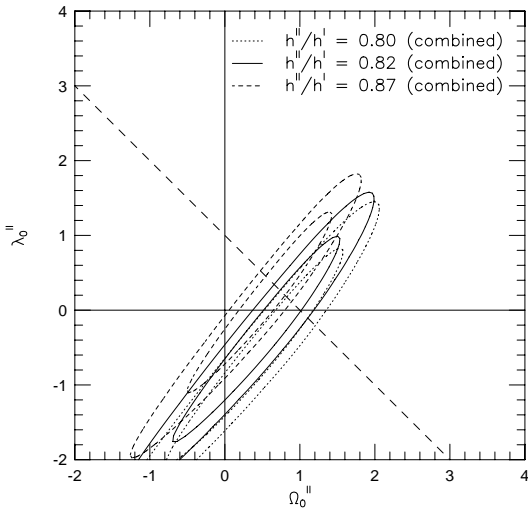


**Figure 4.** 68.3 % and 95.4 % confidence contours in the  $\Omega_0^{\text{II}} - \lambda_0^{\text{II}}$  plane for the combined data. The dotted lines, solid lines and dashed lines represent the cases of  $H_0^{\text{II}}/H_0^{\text{I}} = 0.80, 0.82$ , and  $0.87$ , respectively.

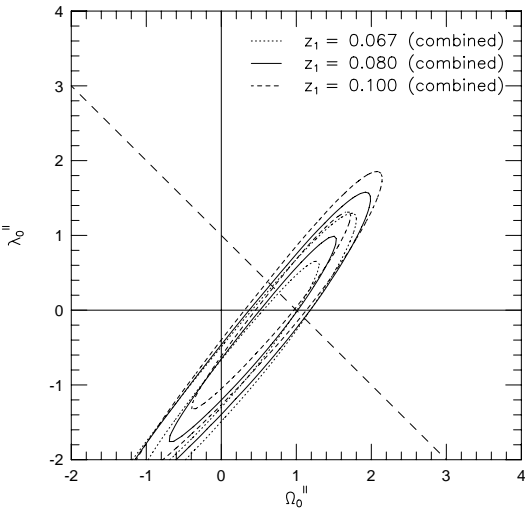


**Figure 5.** 68.3 % and 95.4 % confidence contours in the  $\Omega_0^{\text{II}} - \lambda_0^{\text{II}}$  plane for the combined data. The dotted lines, solid lines and dashed lines represent the cases of  $z_1 = 0.067, 0.080$ , and  $0.100$ , respectively.

$\lambda_0^{\text{II}}$  with  $1\sigma$  error bars, and the corresponding  $\chi_{\nu}^2$  in cases of  $H_0^{\text{II}}/H_0^{\text{I}} = 0.82, 0.87$  and  $0.80$ , respectively, assuming  $z_1 = 0.080$  and  $\Omega_0^{\text{I}}$  (A). The error bars of  $h^{\text{I}}$  include only statistical errors, but not the contribution from the errors of absolute magnitudes.  $\chi_{\nu}^2$  in Perlmutter et al. data is found to be much larger than that in Riess et al. data. This comes from the situation that we made artificially their data of  $\mu_0$  assuming the average absolute magnitude. In Riess et al. data  $\chi_{\nu}^2$  in our inhomogeneous models is smaller than that in homogeneous models (Table 1) and so this data are more fitted to our inhomogeneous models or the inhomogeneity of Hubble constant. To the bottom of Table 1, we add  $(\Omega_0^{\text{II}})_{\text{flat}}$ , the density parameter in the case when the outer region is spatially flat.

In Table 5 we show the best-fit values in the case of  $\Omega_0^{\text{I}}$  (B), assuming  $H_0^{\text{II}}/H_0^{\text{I}} = 0.82$ ,  $z_1 = 0.080$ . From comparison

between Table 2 and Table 5, the best-fit values are not sensitive to  $\Omega_0^{\text{I}}$ . In Table 6, moreover, we show the cases with  $z_1 = 0.067$  and  $0.100$  assuming  $H_0^{\text{II}}/H_0^{\text{I}} = 0.82$  and  $\Omega_0^{\text{I}}$  (A). It is found from this Table that, because of the smallest  $\chi_{\nu}^2$ , the fitting for  $z_1 = 0.080$  is best, compared with the cases with  $z_1 = 0.067$  and  $0.100$ . This result may be connected with the situation that the boundary radius of the observed local void is likely to be between  $200/h^{\text{I}}$  Mpc and  $300/h^{\text{I}}$  Mpc.

#### 4 CONCLUDING REMARKS

In this paper we derived confidence contours and best-fit parameters in the inhomogeneous models with a local void using the two SNIa data and the combined data, and found

that (1) they are very sensitive to the ratio  $R$  of the outer Hubble constant ( $H_0^{\text{II}}$ ) to the inner Hubble constant ( $H_0^{\text{I}}$ ), (2) the best-fit outer density parameter ( $\Omega_0^{\text{II}}$ ) (and cosmological constant parameter ( $\lambda_0^{\text{II}}$ )) increases (and decreases) with the increase of  $R$ , respectively, and (3) ( $\Omega_0^{\text{II}}, \lambda_0^{\text{II}}$ ) can be (1, 0) for  $R \approx 0.8$ . Accordingly the existence of our local void may solve the puzzling *cosmological-constant* problem.

However we neglected the directional dependence of  $[m, z]$  relation which may be an important factor, especially for nearby SNIa, since magnitudes of SNIa are measured by off-center observers. If the data of angular positions of observed SNIa will be published, the directional dependence can be taken into account and the fitting may be promoted.

The flux averaging proposed by Wang (2000) has not been executed here, but it may be important when many high- $z$  data of  $z > 1.0$  appear, because they would be much affected by lensing effect.

## REFERENCES

Blanton, M. R., Dalcanton, J., Eisenstein, J., Loveday, J., Strauss, M. A., SubbaRau, M., Weinberg, D. H., Anderson, Jr., J. E., et al., astro-ph/0012085

Cole, S., Norberg, P., Baugh, C. M., Frenk, C. S., BlandHawthorn, J., Bridges T., Cannon, R., Colless, M., astro-ph/0012429

Folkes, S., Ronen, S., Price, I., Lahav, O., Colless, M., Maddox, S., Deeley, K., Glazebrook, K., et al., 1999, MNRAS, 308, 459

Hudson, M. J., Smith, R. J., Lucey, J. R., Schlegel, D. J., Davies, R. L., 1999, ApJ, 512, L79

Marinoni, C., Monaco, P., Giuricin, G., Costantini, B., 1999, ApJ, 521, 50

Marzke, R. O., da Costa, L. N., Pellegrini, P. S., Willmer, C. N. A., Geller, M. J., 1998, ApJ, 503, 617

Perlmutter, S., Aldering, G., Goldhaber, G., Knop, R. A., Nugent, P., Groom, D. E., Castro, P. G., Deustua, S. et al. , 1999, ApJ, 517, 565

Riess, A. G., Filippenko, A. V., Challis, P., Clocchiatti, A., Diercks, A., Garnavich, P. M., Gilliland, R. L., et al. , 1998, AJ, 116, 1009

Riess, A. G., Filippenko, A. V., Li, W., Schmidt, B., 2000, AJ, 118, 2668

Shectman, S. A., Landy, S. D., Oemler, A., Tucker, D. L., Lin, H., Kirshner, R. P., Schechter, P. L., 1996, ApJ, 470, 172

Schmidt, B. P., Suntzeff, N. B., Phillips, M. M., Schommer, R. A., Clocchiatti, A., Kirshner, R. P., Garnavich, P., Challis, P., et al. , 1998, ApJ, 507, 46

Tomita, K., 2000a, ApJ, 529, 26; astro-ph/9905278

Tomita, K., 2000b, ApJ, 529, 38; astro-ph/9906027

Tomita, K., 2001a, Prog. Theor. Phys., 105, 419; astro-ph/0005031

Tomita, K., 2001b, astro-ph/0011484

Wang, Y., 2000, ApJ, 536, 531

Willick, J. A., 1999, ApJ, 522, 647

Zucca, E., Zamorani, G., Vettolani, G., Cappi, A., Merighi, R., Mignoli, M., MacGillivray, H., Collins, C. et al. , 1997, A&A, 326, 477